Available online at www.sciencedirect.com
ScienceDirect
Journal of the European Ceramic Society 31 (2011) 231–235
www.elsevier.com/locate/jeurceramsoc

Technical note

Microstructure homogeneity control in spark plasma sintering of Al_2O_3 ceramics

Cao Wang [a], Xin Wang [a,b], Zhe Zhao [a,*]

[a] *Department of Materials and Environmental Chemistry, Stockholm University, S-10691 Stockholm, Sweden*
[b] *School of Science, Hangzhou Dianzi University, Hangzhou, Zhejiang 310018, People's Republic of China*

Received 1 July 2010; received in revised form 5 August 2010; accepted 10 August 2010
Available online 15 September 2010

Abstract

Homogeneous microstructure control in the SPS (spark plasma sintering) sintered big size Al_2O_3 ceramic was realized by the synergy effect of grain boundary tailoring and proper pressure profile design. Two-step pressure profile itself did not show any efficient densification enhancement if no grain boundary modifier MgO added. The two-step pressure profile can effectively reduce average grain size and grain size difference over the sintered specimen, while MgO doping can reduce the average grain size in the whole sintered samples. Finally, a general strategy to overcome the intrinsic temperature gradient in SPS is suggested.

Keywords: Sintering; Al_2O_3; Homogeneous microstructure; Grain size

1. Introduction

Nowadays, spark plasma sintering (SPS) is widely accepted as an efficient sintering technique in terms of densification enhancement and grain growth control. Especially for the fine-grained microstructure, SPS has shown excellent competence in different ceramic materials.[1–3] To realize the positive impact of SPS on the mechanical and optical properties, limited or controllable grain growth is critical, thus temperature, heating rate, dwelling time and pressure are always considered as the key factors to be optimized.[4–9]

However, one critical limit for most SPS research is the very limited sample size (diameter <30 mm) and shape achieved in laboratory experiments. For large size ceramic pieces production, both average grain size and microstructure homogeneity need to be seriously evaluated. So far only a few brief investigations on microstructure homogeneity have been reported. Wang et al.[10] noticed that the microstructure inhomogeneity in Al_2O_3 sintered bodies by SPS, but no resolution was suggested. Tuan and co-workers[11] found the temperature variation within ceramic powders compact by careful examination in the phase transformation of gamma-Al_2O_3 at different positions in their SPS sintered samples. It was suggested that a carbon paper between graphite punch and mold or reduced heating rate can significantly reduce the temperature variation. Jayaseelan et al.[12] suggested that very low compaction pressure during SPS will lead to low density and undesirable microstructure inhomogeneity due to differential sintering. Grasso et al.[13] found that the external pressure in SPS played an intrinsic and key role to influence the overall bulk heat generation, thus the microstructure can be affected. High pressure led to more uniform microstructure in the conductive WC materials. Unfortunately, all these studies mainly concern the practical operation parameters other than sintering kinetic process itself. Furthermore, the intrinsic temperature gradient in SPS confirmed by different FEM modeling works[14–16] indicated that it was quite common to have a temperature difference on the level of up to 100 °C, depending mainly on the sintering temperature, in the sintered powder compact. Considering the accumulative effect during the continuous sintering process, it is reasonable to expect serious nonuniformity in microstructure after sintering, especially for most insulator ceramic materials. It is necessary to explore the strategic approaches which can be commonly applied to overcome the potential negative impact of temperature gradient.

The primary goal of this study was to develop a general synergy strategy that allow us to demonstrate the importance of

* Corresponding author. Tel.: +46 8162417; fax: +46 8152187.
E-mail address: zhe.zhao@mmk.su.se (Z. Zhao).

0955-2219/$ – see front matter © 2010 Elsevier Ltd. All rights reserved.
doi:10.1016/j.jeurceramsoc.2010.08.015

materials design, more straightforward to say grain boundary passivation by doping, except for the proper sintering parameter selection. So a two-step pressure profile and MgO doping are applied for 36 mm Al_2O_3 plates in this study to present the performance of such a strategy.

2. Experimental procedure

Two commercial high-purity α-Al_2O_3 powders (purity >99.99%, Taimicron TM-DS, Taimei Chemical Co., Ltd., Tokyo, Japan) were used in this study. One pure powder (DS-81) and another doped with 500 ppm MgO (DS-90M), with a mean particle size of 0.1 μm and specific surface is of 13.5 m^2/g. They are hereafter designated as pure and MgO doped powders, respectively. In order to avoid any carbon residues after SPS sintering, organic binders were removed through calcination at 650 °C for 2 h.

Sintering was carried out in vacuum (4–6 Pa) with a Dr. Sinter 2050 spark plasma sintering (SPS) apparatus (Sumitomo Coal Mining Company Ltd., Tokyo, Japan). The as-received powder was loaded into a cylinder-shaped graphite die with an inner diameter of 36 mm. The temperature was increased to 600 °C within 4 min and then further increased to 1300 °C in 7 min; the final stage of heating to 1350 °C was finished in 1 min; and held at 1350 °C for 5 min. There are two type of pressure profile were used: (a) 1-step pressure profile, where a constant uniaxial pressure of 100 MPa was loaded in the whole sintering process and (b) 2-step pressure profile, where a uniaxial pressure of 20 MPa was loaded and kept constant till 1300 °C and then the pressure was increased to 100 MPa in 1 min and kept constant till the end of the sintering. Both temperature and pressure are controlled through a programmable interface. The evolution of both temperature and pressure as a function of time for two sintering cycles is clearly plotted in Fig. 1a. Namely, all specimens were sintered at 1350 °C for 5 min with 100 MPa. More detailed experimental conditions for four different samples can be found in Table 1.

Density was measured by Archimedes' method using water as the medium and 3.989 g/cm^3 was used as theoretical density for relative density calculation. The microstructure investigation was carried out using a FE-SEM (JSM-7000F, JEOL, Japan) on the polished and thermally etched cross-section surface (1100 °C, in air, 2 h). The grain size d was estimated by the intercept-line measurement on at least 200 grains, a correction factor of 1.56[17] was applied.

Table 1
Specimen designation, sintering conditions, and relative density of the SPSed-Al_2O_3 ceramics.

Specimen designation	Starting powder	T (°C)	Pressure profile	Relative density (%)
Pure-1	Pure	1350	1-step	98.2
Pure-2	Pure	1350	2-step	98.3
Mg-1	MgO doped	1350	1-step	98.6
Mg-2	MgO doped	1350	2-step	99.5

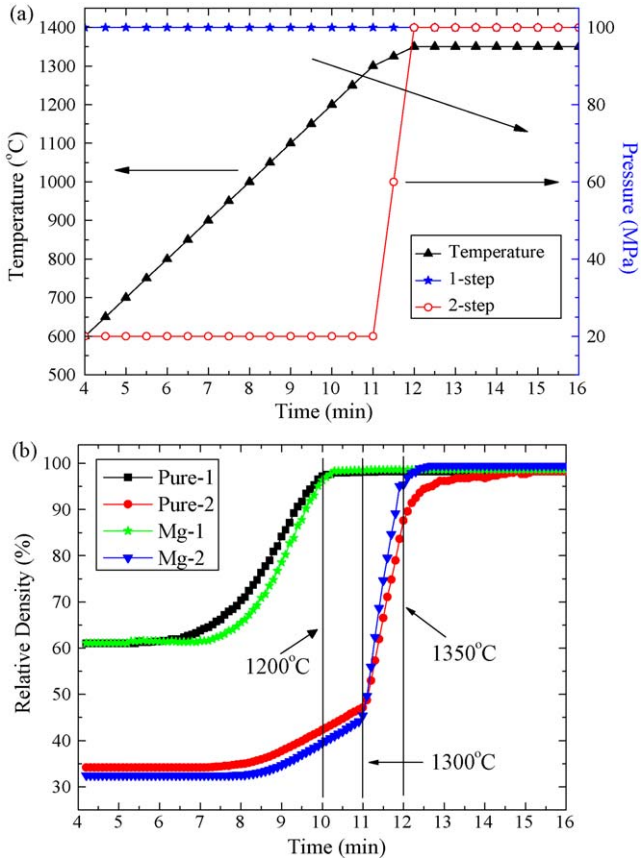

Fig. 1. The evolution of temperature, pressure and relative density as the function of time in two sintering cycles.

3. Results and discussion

For any sintering process, densification and grain growth are always two interacted processes and so they need to be simultaneously considered for better understanding with any specific sintering technique. As shown in Table 1, among the four samples sintered at the same temperature and time, Mg-2 sample shows noticeably higher density than other three samples. All other three samples show relatively low density compared ones in our previous experiments, where the same powders and sintering conditions but a smaller size of 12 or 20 mm diameter samples can be easily sintered to be very close to fully dense (>99.5% RD). Compared with the 20 mm samples prepared by Jayaseelan et al.[12], which are consolidated to 99% from the similar starting powder and lower sintering temperature (1250 °C) and lower pressure (15 MPa), pure-1, pure-2 and Mg-1 are obviously inferior to their results too. The relatively poor densities indicate that big size samples preparation definitely suffers the difficulties in the densification. Except for the Mg-2 sample, which was prepared from 500 ppm MgO doped Al_2O_3 powder and 2-step pressure profile, all other three samples meet the difficulty to have efficient densification, even with SPS such an special sintering technique. It is noteworthy that there is no notable difference in density between pure-1 and pure-2, while notable difference between Mg-1 and Mg-2 can be found. So it can be concluded that 2-step pressure profile will not make

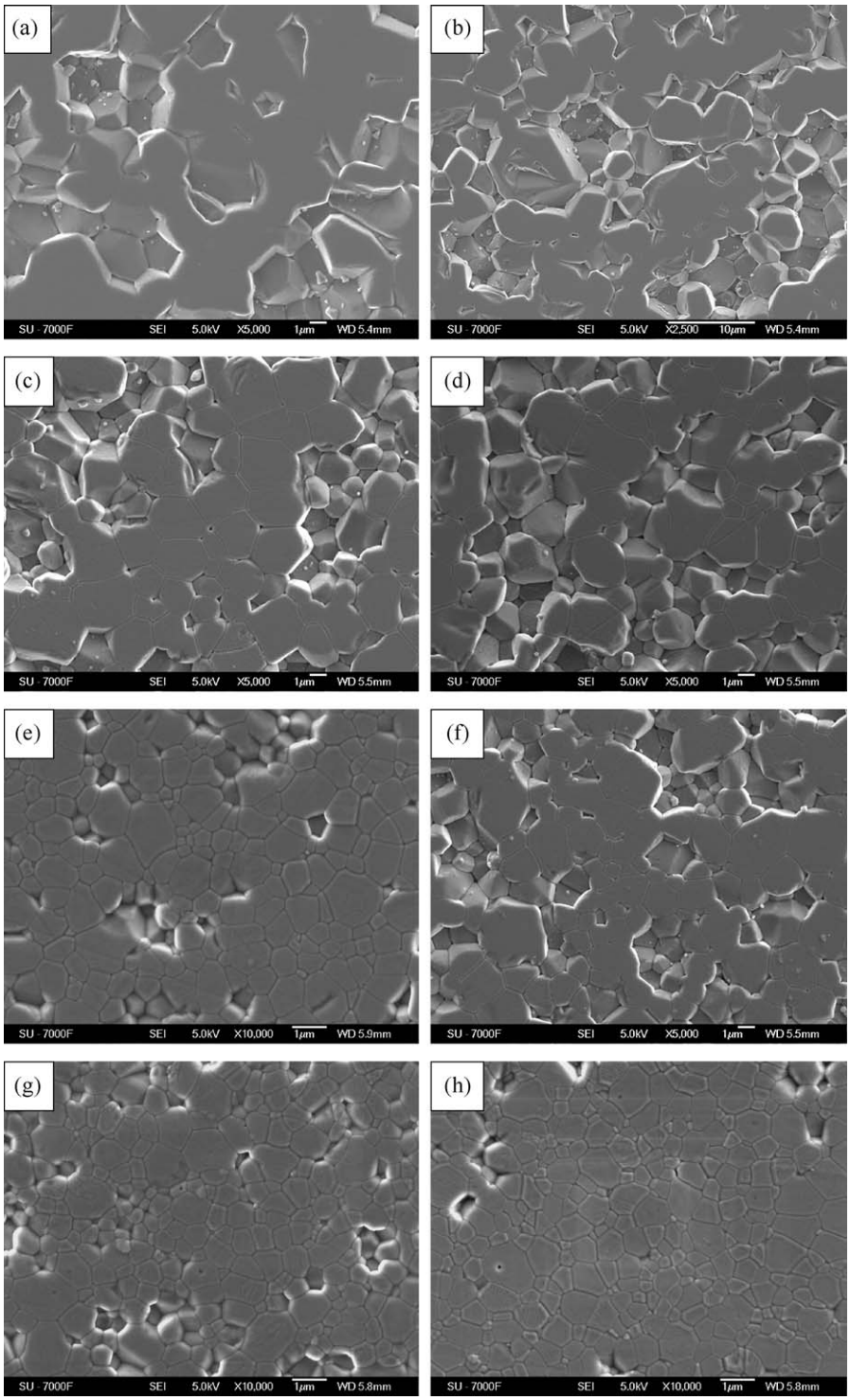

Fig. 2. The microstructure at the edge (a, c, e, g) and center (b, d, f, h) part for pure-1 (a and b), pure-2 (c and d), Mg-1 (e and f) and Mg-2 (g and h) 36 mm Al_2O_3 plates.

dramatic change in the densification of pure Al_2O_3, but 2-step pressure profile indeed enhance the densification in MgO doped Al_2O_3.

To understand such an effect better, the relative density development during SPS in all four samples are presented in Fig. 1b. Due to the densification enhancement by external high pressure of 100 MPa, all 1-step pressure profile samples show much higher density before the final dwelling period. Pure-1 even shows higher density than Mg-1 when the same moment (temperature) is taken. The presence of MgO even prevents the densification process in high-purity Al_2O_3 before reaching the final density limit, where temperature is still low (<1200 °C). For temperatures >1200 °C, however, the relative density curves for pure-1 and Mg-1 start to be totally overlapped. This indicates

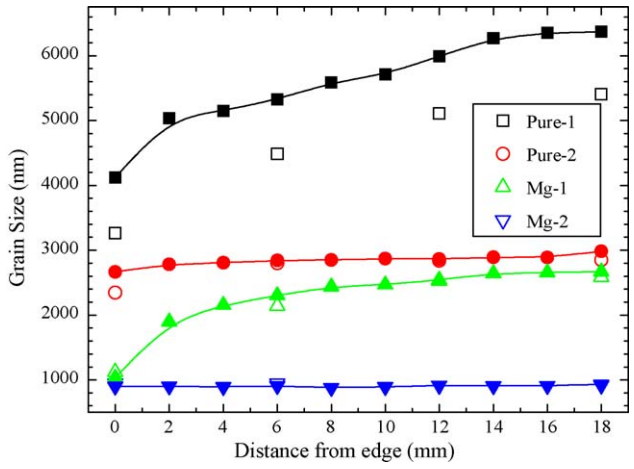

Fig. 3. The grain size distribution along radial direction for SPS sintered samples. Solid marks are for the middle line parallel to the sample surface; unfilled marks are for the positions very close to the sample surface.

that the MgO doping linked densification mechanism is highly favoured by high temperature. With the increase of temperature, the densification in Mg-1 gradually catches up with that in pure-1. On the contrary, the presence of MgO in 2-step pressure profile samples obviously enhances the densification process after the increase of pressure at temperatures higher than 1300 °C, Mg-2 always shows higher density than pure-2 in the sintering period after 1300 °C. This, again demonstrates that the existence of MgO enhance the SPS densification process in Al_2O_3 at high temperatures. Due to the fact that the external pressure will introduce extra densification contribution of deformation, the extra contribution of grain boundary sliding induced shrinkage make the densification process more efficient. In the case of 2-step pressure profile, the very low density (45% RD) and high temperature (1300 °C) at the moment of increasing pressure make the plastic deformation much easier in both pure-2 and Mg-2. But Mg-2 get even more contribution of deformation due to the existence of grain boundary energy modifier MgO.

To carefully investigate the microstructure homogeneity in all different samples, high quality SEM images were taken at different positions and grain size distribution along the radial direction was quantified. In Fig. 2, SEM images give direct evidence for the microstructure homogeneity. Pure-1 and Mg-1 clearly show dramatic difference in grain size between the center and edge. Once the 1-step pressure profile was applied, such a grain size inhomogeneity is inevitable. But the degree of the inhomogeneity in Mg-1 is less that in pure-1. For 2-step pressure profile samples, pure-2 and Mg-2, the microstructure homogeneity has been improved over the 1-step samples. 2-step pressure profile is obviously very efficient to improve the microstructure homogeneity. This is also in good agreement with our previous work with transparent $MgAl_2O_4$.[9] It can be also found that 2-step pressure profile is effective to reduce the average grain size due to the much shorter heating history for high density range, where grain growth is the dominating process during the final sintering stage. Comparing pure-1 and Mg-1, pure-2 and Mg-2, the presence of MgO is good for grain growth control over the whole sintered sample. In Fig. 3, more solid quantitative data of grain size distribution are presented for all four samples. Generally, MgO doping reduces grain size over the whole sintered plate but doesn't help to get rid of the microstructure inhomogeneity; 2-step pressure profile can effectively get rid of the microstructure inhomogeneity problem in the samples investigated here. To further investigate the microstructure homogeneity in the direction parallel to the pressure application, several positions very close to the top surface of the samples are also analysed and the quantitative results are represented as the unfilled marks in Fig. 3. It can be found that the inhomogeneity exists in all directions and so it can be eliminated at the same time. The combination of 2-step pressure profile and 500 ppm MgO doping leads to a fine-grained and homogeneous 36 mm plate, which is actually translucent while the other samples are totally whitish. A highly transparent and homogeneous big size Al_2O_3 window can be anticipated if further optimization with powder processing can be done in the near future.

As we mentioned earlier, the temperature gradient is the intrinsic problem for SPS and this cannot be avoided by simply changing sintering parameters even we agree that it can be alleviated by proper selection of SPS parameters, e.g. two-step profile. But as shown in this work, single two-step pressure profile cannot guarantee submicron grain size at high temperature even the homogeneity can be improved. A more fundamental strategy to make ceramic materials inert to temperature and to keep fine and homogeneous microstructure is needed. For this purpose, based on the results presented in this study, to make a grain boundary movement passivation in wider temperature range will be more critical and can be regarded as the fundamental strategy. Grain boundary segregation and solute drag effect by Mg[18] and other elements[19] can reduce grain boundary mobility and therefore help to obtain more homogeneous microstructures in sintering. The synergy effect of grain boundary tailoring by doping and proper pressure profile design has been demonstrated here as one good example to realize such a strategy.

4. Conclusions

It has been shown that a dense and homogeneous fine-grained Al_2O_3 can be achieved by a combination of 500 ppm MgO doping and 2-step pressure profile in SPS sintering process. Two-step pressure profile not only reduces the average grain size but also improve the uniformity of the grain size over the whole sintered sample. As an addition and important strategy, grain boundary passivation by MgO doping can limit the grain growth while alleviate the microstructure inhomogeneity. To avoid the negative influence of the intrinsic temperature gradient in SPS need both proper sintering parameters selection and grain boundary doping.

Acknowledgments

This study was supported by the grant through EU 6th FP IP-Nanoker project (NMP3-CT-2005-515784). We also would like to appreciate the EM facility support from Knut and Alice Wallenberg Foundation.

References

1. Groza JR. Nanosintering. *Nanostruct Mater* 1999;**12**:987–92.
2. Zhao Z, Buscaglia V, Bowen P, Nygren M. Spark plasma sintering of nanocrystalline ceramics. *Key Eng Mater* 2004;**264–268**:2297–300.
3. Zhao Z, Buscaglia V, Viviani M, Buscaglia MT, Mitoseriu L, Testino A, et al. Grain-size effects on the ferroelectric behavior of dense nanocrystalline $BaTiO_3$ ceramics. *Phys Rev B* 2004;**70**:024107.
4. Shen Z, Johnsson M, Zhao Z, Nygren M. Spark plasma sintering of alumina. *J Am Ceram Soc* 2002;**85**:1921–7.
5. Stuer M, Zhao Z, Aschauer U, Bowen P. Transparent polycrystalline alumina using spark plasma sintering: effect of Mg, Y and La doping. *J Eur Ceram Soc* 2010;**30**:1335–43.
6. Kim B-N, Hiraga K, Morita K, Yoshida H. Spark plasma sintering of transparent alumina. *Scripta Mater* 2007;**57**:607–10.
7. Jiang DT, Hulbert DM, Anselmi-Tamburini U, Ng T, Land D, Mukherjee AK. Optically transparent polycrystalline Al_2O_3 produced by spark plasma sintering. *J Am Ceram Soc* 2008;**91**:151–4.
8. Anselmi-Tamburini U, Woolman JN, Munir ZA. Transparent nanometric cubic and tetragonal zirconia obtained by high-pressure pulsed electric current sintering. *Adv Funct Mater* 2007;**17**:3267–73.
9. Wang C, Zhao Z. Transparent $MgAl_2O_4$ ceramic produced by spark plasma sintering. *Scripta Mater* 2009;**61**:193–6.
10. Wang SW, Chen LD, Hirai T, Guo JK. Formation of Al_2O_3 grains with different sizes and morphologies during the pulse electric current sintering process. *J Mater Res* 2001;**16**:3514–7.
11. Zhang D, Zhang L, Guo J, Tuan W-H. Direct evidence of temperature variation within ceramic powder compact during pulse electric current sintering. *J Am Ceram Soc* 2006;**89**:680–3.
12. Jayaseelan DD, Ueno S, Ohji T, Kanzaki S. Differential sintering by improper selection of sintering parameters during pulse electric current sintering. *J Am Ceram Soc* 2004;**87**:159–61.
13. Grasso S, Sakka Y, Maizza G, Hu C. Pressure effect on the homogeneity of spark plasma-sintered tungsten carbide powder. *J Am Ceram Soc* 2009;**92**:2418–21.
14. Wang YC, Fu ZY. Study of temperature field in spark plasma sintering. *Mater Sci Eng B* 2002;**90**:34–7.
15. Wang X, Casolco SR, Xu G, Garay JE. Finite element modeling of electric current-activated sintering: the effect of coupled electrical potential, temperature and stress. *Acta Mater* 2007;**55**:3611–22.
16. Wang C, Cheng LF, Zhao Z. FEM analysis of the temperature and stress distribution in spark plasma sintering: modelling and experimental validation. *Comput Mater Sci* 2010;**49**:351–62.
17. Mendelson MI. Average grain size in polycrystalline ceramics. *J Am Ceram Soc* 1969;**52**:443–6.
18. Powers JD, Glaeser AM. Grain boundary migration in ceramics. *Interface Sci* 1998;**6**:23–39.
19. Yoshida H, Ikuhara Y, Sakuma T. Grain boundary electronic structure related to the high-temperature creep resistance in polycrystalline Al_2O_3. *Acta Mater* 2002;**50**:2955–66.